



Orthogonally polarized and 60 GHz dual-channel based 18×2.5 Gb/s DWDM-interleaved hybrid FSO system under atmospheric turbulence

Abhishek Tripathi¹ · Shilpi Gupta¹ · Abhilash Mandloi¹

Received: 6 August 2019 / Accepted: 23 March 2020 / Published online: 10 April 2020
© Springer Science+Business Media, LLC, part of Springer Nature 2020

Abstract

This paper proposes an optical distribution system by integrating free space optics/passive optical network and radio over free space optics in a dense wavelength division multiplexing architecture. In this approach, the system adopts generation of dual 60 GHz bands, two orthogonal states of polarization (SOP) and wavelength-interleaving scheme. This improves spectral efficiency by facilitating the simultaneous transmission of 6 wired and 12 wireless channels (each at 2.5 Gb/s data rate). This hybrid interleaved signal of 45 Gb/s within 200 GHz spectrum is successfully transmitted over a 400 m free space turbulent atmospheric link. The simulation results show that the mutual SOPs affect equally in performance fluctuations, however, it is found that the intermediate spectral channels/bands have more crosstalk interference compared to neighboring outer channels/bands. At a bit error rate (BER) of 10^{-9} , the receiver sensitivity difference between the wired and wireless services is found in range of ~ 3 to ~ 4 dBm.

Keywords Free space optics · DWDM · Wavelength interleaving · Polarization · Passive optical network · RoFSO · Atmospheric turbulence

1 Introduction

FSO system has become an important research topic as it can provide easy-to-install practical links, isolation from electromagnetic interference, unlicensed bandwidth, prominent solution for multi-services wireless network and the promise of similar data capacity to that of optical fiber-based communication (Ciaramella et al. 2009; Mallick et al. 2019; Tsai et al. 2015). In cities where infrastructure developments (i.e. roads and underground infrastructures) have already been done, telecommunication companies are facing challenges in laying optical fiber (Majumdar 2014). Therefore, FSO installation is an alternative link

✉ Abhishek Tripathi
tripathi.abhishek.5@gmail.com

Shilpi Gupta
shilpig1980@gmail.com

¹ Department of Electronics Engineering, Sardar Vallabhbhai National Institute of Technology, Surat, Gujarat 395007, India

between the buildings/towers or a backup to fiber cables in inaccessible areas (Kim and Korevaar 2001). If the FSO network is made to be spread over the existing PON in an urban area, then, the FSO/PON (or FSO-FTTH) scenario would definitely be more beneficial as the dedicated running fiber is already laid down serving the bandwidth-intensive applications such as high definition television (HDTV) or video on demand (Aldouri et al. 2013; Mandal et al. 2017). Typically, a WDM-PON connects a multiwavelength optical line terminal (OLT) to multiple end users at the side of an optical network unit (ONU) through a fiber to the home (FTTH) link (Dayal et al. 2017). It would be better to replace fiber in traditional PON with FSO link in areas where it faces terrestrial difficulties and cost-ineffectiveness (Badar et al. 2018; Zhang and Ma 2017), though, the reduced channel spacing in DWDM-FSO system becomes vulnerable to weather and atmospheric turbulence-induced fading (Badar and Jha 2017).

Recently, significant progress has been made on RF/wireless access technologies because they are more convenient, scalable, and resilient for roaming connections (Ghosh et al. 2005; Mallick et al. 2018; Mandal et al. 2018). As FSO communication is evolving to transmit RF signals, which are similar to radio over fiber (RoF) but excluding the fiber which is referred to as RoFSO (Chaudhary et al. 2018; Ni et al. 2009). The integration of FSO/PON carrying baseband signal with RoFSO system may yield a cost-effective hybrid optical access solution to serve both fixed and mobile users without any change of optical line terminal (OLT) configuration (Yeh et al. 2018). It is expected that the millimeter-wave (mm-wave) bands would be utilized to meet the requirement to overcome the frequency congestion in the future wireless access networks (Sharma and Kaur 2013). Allocation of the mm-wave band (57–64 GHz band in USA and 59.0–66.0 GHz in Japan) as unlicensed spectrum is growing interest worldwide (Yong et al. 2011). Despite high atmospheric loss, the continuing trend in most applications are moving to 60 GHz (standardized as 'IEEE 802.11ad') to establish gigabit links for home and personal area network (Giannetti et al. 1999). In an evolution of broadband wireless access system, RoFSO system is capable of transmitting multiple RF signals. Recently, numerous methods have been reported related to photonic generation of mm-wave (Devgan et al. 2015; Yu et al. 2005). Among these methods, Mach-Zehnder modulator (MZM) could be used to generate single or multi-mm-wave bands which carries RoFSO signals (Hsueh et al. 2009).

Since FSO technology is still evolving at a relatively faster rate, possible optical distribution design continues to evolve towards merging of multiple services in a single shared infrastructure (Mandal et al. 2017). Thus, compared to the independent architectures of RoFSO and WDM-PON, this hybrid architecture is expected to improve the overall system performance in terms of QoS for new-generation wired and wireless accesses (Li et al. 2009). Depending on the deployment scenario and application, FSO/PON and RoFSO based OLT can be easily upgraded by adopting further innovative schemes such as (1) polarization division multiplexing (PDM) and (2) optical interleaving (Bakaul et al. 2005). The combination of PDM along with WDM allows efficient utilization of the available optical bandwidth in polarization and wavelength domains. In free space, two orthogonal SOPs are a better choice to maintain their state of polarization while propagating in free space (Hayee et al. 2001). However, SOP orthogonality is degraded due to optical components used at the transceiver side. The concept of optical frequency interleaving was proposed to increase the spectral efficiency of the system. The optical carriers and their respective modulation sidebands are interleaved in such a way that the adjacent channel spacing is utilized with minimum crosstalk interference.

This paper mainly focuses on photonic integration of FSO-FTTH and RoFSO techniques. To the best of our knowledge, a typical method for generating dual 60 GHz bands has also not

been introduced in the previous literatures. The data capacity of the hybrid signal is increased by interleaving of polarized DWDM channels. An illustration of a proposed FSO system is depicted in Fig. 1, where hybrid data is distributed from OLTs to ONU nodes through the terrestrial atmospheric link. In each ONU, the signal in the central carrier is used for wired service and frequency band is utilized for the wireless service.

The paper is organized as follows. The effect of atmospheric turbulence on the performance of FSO link is described theoretically in Sect. 2. Demonstration of the proposed design for simultaneous delivery of dual services over hybrid optical distribution link is presented in Sect. 3. Simulation results are covered in Sect. 4. Finally, Sect. 5 concludes this paper.

2 Effect of atmospheric turbulence

Inhomogeneous temperature and wind pressure fluctuations in free space lead to variations in the refractive index. This resultant impairment in the FSO system is called as atmospheric turbulence, which further manifests scintillation (Soni et al. 2019; Tripathi et al. 2019). It causes the random fluctuations of the phase and intensity of the received signal thus degradation of the system performance. Let $n(\rho_1)$ and $n(\rho_2)$ be values of the R.I. at the vector location ρ_1 and ρ_2 respectively, therefore R.I. fluctuation in term of refractive index structure function D_n is defined in Eq. 1 (Majumdar and Ricklin 2010):

$$D_n(\rho_1, \rho_2) = \langle |n(\rho_1) - n(\rho_2)|^2 \rangle \tag{1}$$

Where $\langle \dots \rangle$ represents statistical averaging, as D_n depends only on modulus of the vector separation $\rho = \rho_1 - \rho_2$, so $D_n(\rho_1, \rho_2)$ can be rewritten $D_n(\rho)$. It is described by the Kolmogorov-Obukhov 2/3 power law for the optical turbule sizes bounded by the inner scale l_o and outer scale L_o (Kaushal et al. 2011):

$$D_n(\rho) = C_n^2 \rho^{2/3} \quad \text{at } l_o < \rho < L_o \tag{2}$$

where, the proportionality constant C_n^2 is called index of refraction structure parameter, and it characterizes the amount of refractive index fluctuation consequently strength of turbulence. C_n^2 can be defined as:

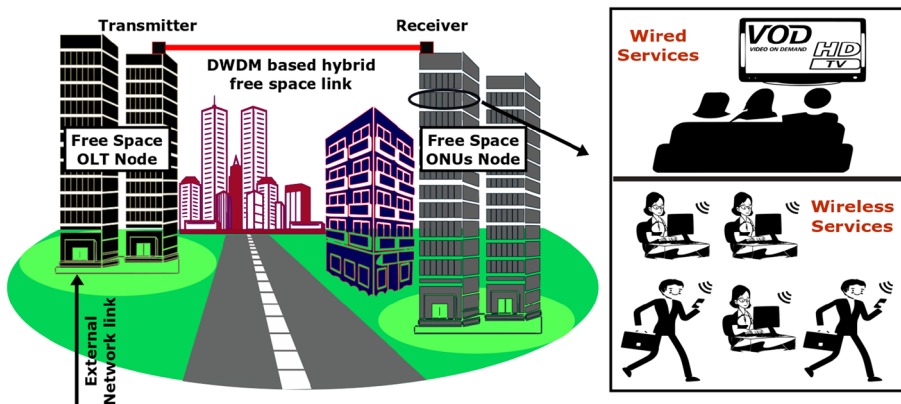


Fig. 1 An optical distribution scenario of wired and wireless signal over a single terrestrial FSO link

$$C_n^2 = \left(86 \times 10^{-6} \times \frac{P}{T^2} \right)^2 C_T^2 \tag{3}$$

where, P is pressure in millibars, T is temperature in Kelvin and C_T is temperature structure parameter as given by (Kaushal et al. 2011):

$$C_T = \sqrt{\langle \delta T^2 \rangle} r^{-1/3} \tag{4}$$

where, δT is temperature gradient and r is the distance between points at which temperatures are measured.

The value of C_n^2 varies with the turbulence strength that categorizes the turbulence regimes. C_n^2 typically ranges from $10^{-12} m^{-2/3}$ to $10^{-17} m^{-2/3}$ for strong to weak turbulence (Ghassemlooy et al. 2019).

3 System configuration

In the schematic setup as shown in Fig. 2, the case of first OLT design is as follows.

The 1549.59 nm from distributed feedback laser (DFB1) having a linewidth of 10 MHz and power of 3 mW (Fig. 3a) is modulated by a Dual-Drive Mach-Zehnder Modulator (DD-MZM1) with the sinusoid wave of 20 GHz and 40 GHz (modulating voltage = 1.9 and 2.1 respectively). It leads to the generation of two sub-bands of 40 GHz and 80 GHz, where the sidebands are equally spaced from the central wavelength. The extinction ratio of DD-MZM is fixed at 11 dB and the bias point is adjusted to 3V to make all five spectral

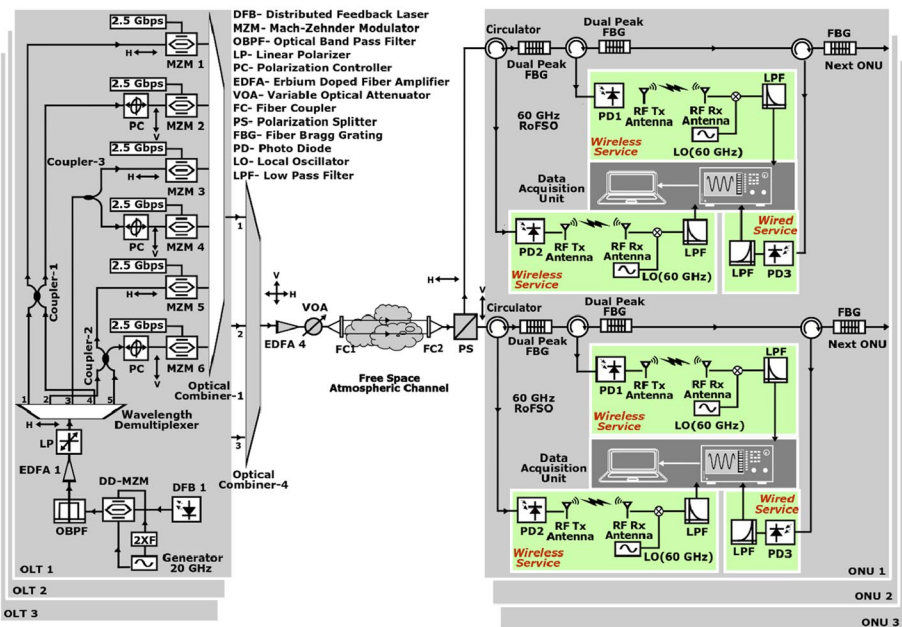


Fig. 2 Schematic setup of proposed hybrid transmission providing wired and wireless connectivity through the free space atmospheric link

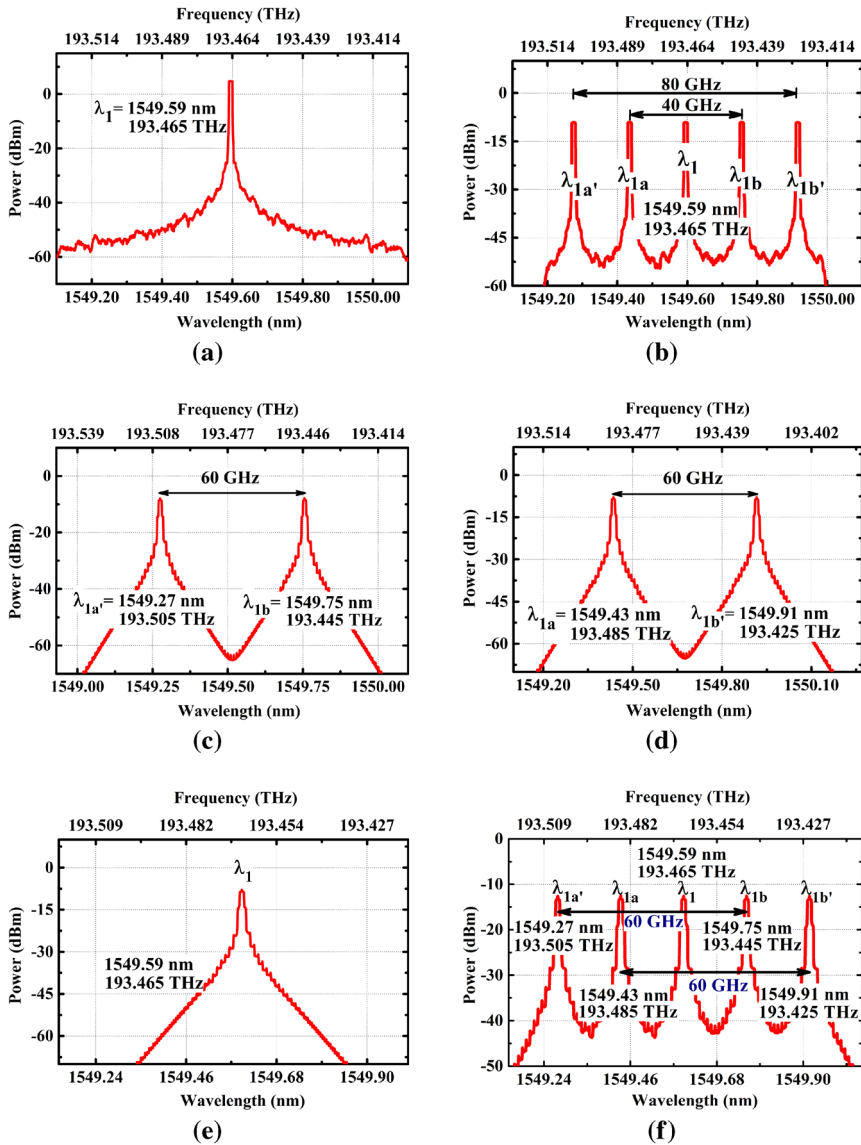


Fig. 3 Optical spectra of **a** DFB1 output, **b** photonic generation of dual mm-wave bands, **c**, **d** 60 GHz mm-bands carrying RoFSO signal **e** modulated central carrier with baseband signal **f** composite signal after optical combiner-1

peaks flat with equal power (Fig. 3b) These channel/bands pass through optical band-pass filter (OBPF), and will see a large penalty for narrow optical filtering effects. Therefore, an erbium doped fiber amplifier (EDFA1) is used to boost the optical power with a gain of 10 dB (noise figure = 4 dB). All 20 GHz equally spaced spectral components are made to be horizontally polarized (0°) by the linear polarizer (LP). All the channel/bands undergo through a 1×5 demultiplexer (0.5-dB bandpass bandwidth of 20 GHz and channel

isolation of 24 dB). Demultiplexed output from terminal no. 1 and 4 are coupled with coupler-1, 2 and 5 are coupled with coupler-2, and 3 with coupler-3. The each coupler is having coupling coefficient = 0.5 and insertion loss = 0.2 dB.

The output of these couplers provides the formation of two sets of 60 GHz sub-carrier bands associating with central carriers. One output from each coupler gets converted to SOP of 90° by polarization controller. Finally, dual-set of 60 GHz orthogonally polarized bands (Fig. 3c, d) will be used for carrying the signal of four wireless users. On the other hand, one set of an orthogonally polarized central carrier (Fig. 3e) will bear two wired services. Therefore, MZM1 to MZM6 (extinction ratio = 30 dB) are used to modulate six 2.5 Gb/s NRZ (PRBS:sequence length = 256) signals. All modulated signals with orthogonal SOPs are obtained at modulator output. Horizontally (Pol-H, azimuth= 0°) and vertically polarized (Pol-V, azimuth = 90°) signals can be visualized on the Poincare sphere in Fig. 4a, b respectively. The Stokes parameters are measured as $[S1, S2, S3] = [1, 0, 0]$ for Pol-H and $[S1, S2, S3] = [-1, 0, 0]$ for Pol-V. These signals bearing channels/bands are further combined by optical combiner-1 (Fig. 3f). Consequently, wavelength interleaved signal with an enhanced data capacity of 15 Gb/s is obtained using wavelength-cum-polarization multiplexing.

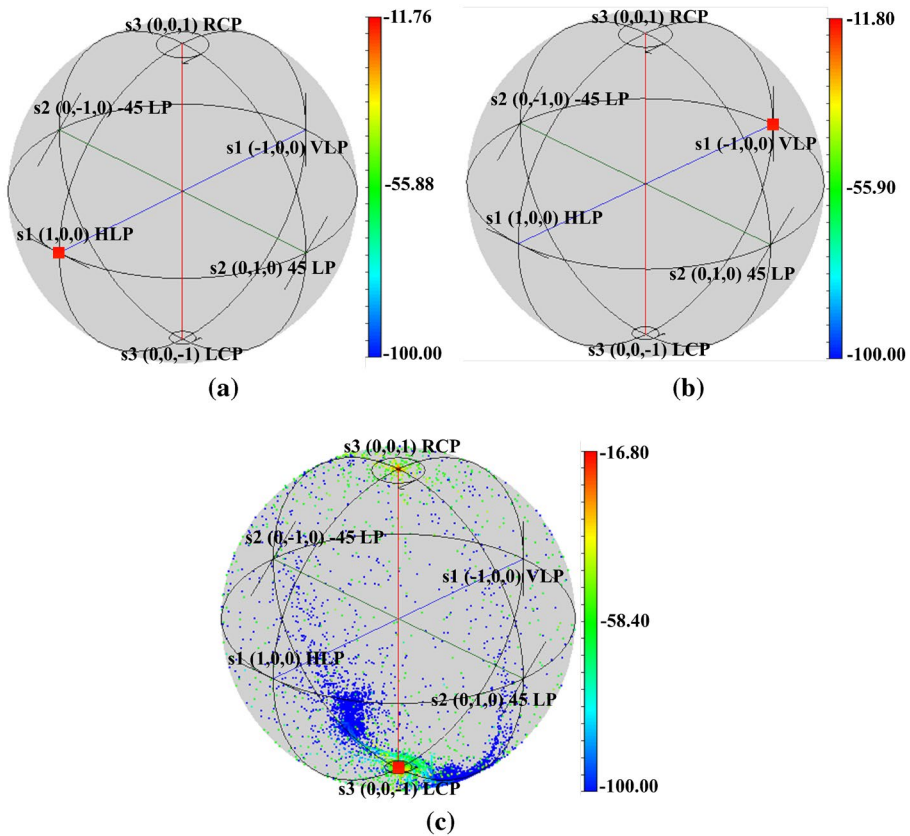


Fig. 4 Spatial distribution of SOPs on the Poincare sphere with color palettes **a** Pol-H, **b** Pol-V: located on equator **c** resultant left-circularly polarized SOP where maximum intensity lies on south pole

The mechanism described earlier is replicated for all OLTs. Since the complete system is proposed for 18 users, therefore, the layout is constructed with DFB1 (1549.59 nm), DFB2 (1549.99 nm) and DFB3 (1550.39 nm), to serve ONU1, ONU2 and ONU3 respectively. A constant offset between two adjacent lasers is set to 0.4 nm (50 GHz). Thus, 3 sets of hybrid signals from combiner-1, 2 and 3 are obtained. Subsequently, such 15 spectral components are obtained when it passes through an optical combiner-4. The resultant hybrid interleaved in Fig. 5a reports successful hybrid interleaving of 15 frequency components. This composite spectrum co-share data of 18 users indicating the possibility of enhancing channel capacity per DWDM channel. The λ_1, λ_2 and λ_3 are the central carriers carrying the baseband signals for wired services while their two sets of associative bands (i) $\lambda_{1a'} - \lambda_{1b}, \lambda_{2a'} - \lambda_{2b}, \lambda_{3a'} - \lambda_{3b}$ and (ii) $\lambda_{1a} - \lambda_{1b'}, \lambda_{2a} - \lambda_{2b'}$ and $\lambda_{3a} - \lambda_{3b'}$ are carrying 60-GHz RoFSO signals for wireless services. The frequency interval between $\lambda_{1a'}$ and $\lambda_{3b'}$

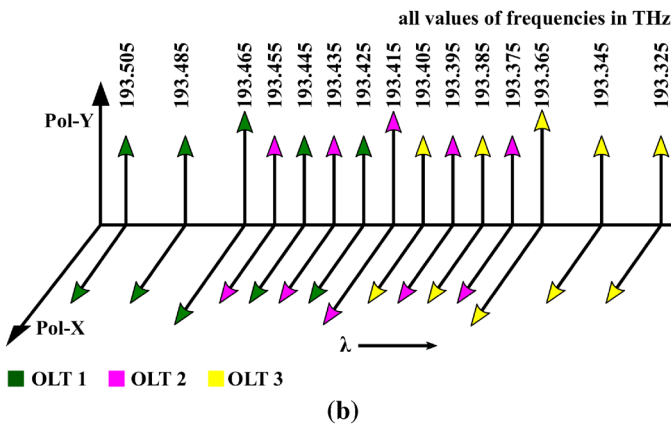
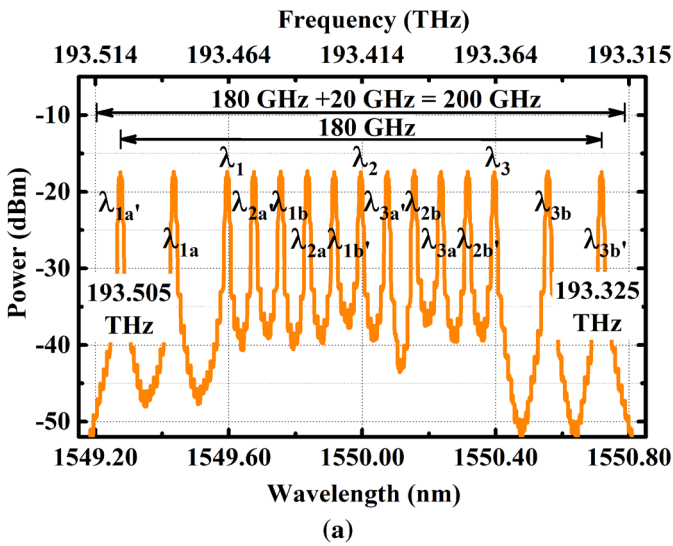


Fig. 5 Interleaving of fifteen frequency components carrying signal of 18 users in **a** frequency domain with spanning spectral band of 200 GHz and **b** state of polarization orthogonality

is 180 GHz. To avoid information loss, an extra margin of 20 GHz is included so that the total spectrum spans within a single DWDM grid of 200 GHz. Figure 5b illustrates the polarization orthogonality of each wavelength which permits to double the user capacity and increase the spectral efficiency. The measured Stokes parameters for a polarized light wave are $[S_1, S_2, S_3] = [-0.005, -0.003, -0.99]$ with azimuth = 73.6 and the ellipticity = -44.8. Its SOP confirms left-circularly polarized light (Fig. 4c), where power is almost equally coupled into the two orthogonal states. Some intermediate polarization (low intensity) points appear on southern sphere of the Poincare sphere due to non-ideal polarization sensitive components used in OLTs.

This signal is boosted by the EDFA to provide additional power penalty for compensating atmospheric attenuation. Moreover, a variable optical attenuator (VOA) is used to change the power level launched from the OLTs. It keeps EDFA pump level same for all measurements with similar noise conditions. The combined signal (total launching power = 15 dBm) is transmitted through fiber collimator (FC1) into 400 m horizontal FSO link, having attenuation = 20 dB/km, beam divergence = 1 mrad and transmitter aperture diameter = 5 cm.

At the receiver end, the transmitted signal is collected by aligned FC2 (aperture diameter = 10 cm). A polarization splitter (PS) splits the received optical signal into Pol-H and Pol-V, before traveling to respective branches. Instead of an optical power splitter, cascaded fiber Bragg grating (FBG) along with circulator are used to demultiplex channels in multiple drop sections. At ONU1, the received hybrid signal along with Pol-H utilizes an FBG to drop the central carrier of 1549.37 nm, and respective bands bearing RF signal is directed down with the help of dual-peak FBG. These reflected signals are received by the separate PIN photodiodes (PD) with responsivity = 1 A/W and dark current = 0.9 nA. The 2.5 Gb/s baseband is directly retrieved by PD3 for wired service. On the other hand, RoFSO signals are detected by PD1 and PD2, produces a 60-GHz signal which is then radiated from the RF antenna to the wireless mobile user in a 50 m radio coverage. The conceptual architecture of the base station was identically realized by proving wireless loss modeled with an electrical attenuator of 2 dB. At the mobile end user, original data of 2.5 Gb/s is recovered by mixing a 60 GHz local oscillator (LO) frequency. Similarly, the detection process was also done with counterpart polarization state (Pol-V). These electrical signals are filtered by low pass filters and the digitization is achieved by using a digital oscilloscope. The captured data is then processed to evaluate communication metrics. The remaining transmitted channels/bands through FBGs will go to next OLTs and provide services to other 12 users in a similar fashion.

4 Results and discussion

The performance of hybrid interleaved FSO link is evaluated in terms of BER (1) as a function of the received optical power and (2) with the variation of C_n^2 . Each plot compares 3 wired and 6 wireless services.

Figures 6 and 7 show the approximately equal power range for Pol-H and Pol-V, which means orthogonal polarization channels are mutually affected in same magnitude. Therefore, BER difference between two polarizations of each channel is negligible. It is also worth noting that when the data passes through subsequent FBGs, signal slightly deteriorates due to unexpected power fluctuations by the individual grating. Hence, ONU1 offers considerably better performance than ONU2 and ONU3.

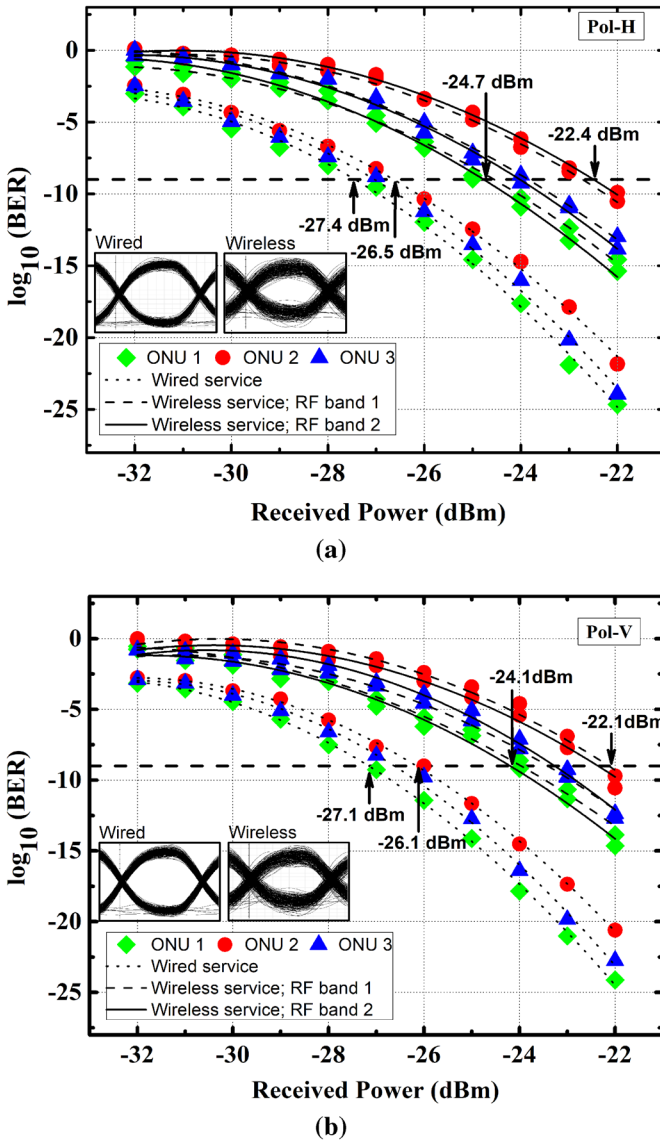


Fig. 6 The BER comparison between wired and wireless services as a function of received optical power for a Pol-H, b Pol-V

In Fig. 6a, b, for typical average turbulence ($C_n^2 = 10^{-15} m^{-2/3}$), the standard BER performance of 10^{-9} is achieved, when minimum to maximum received power lies between -27.4 to -26.5 dBm for Pol-H and -27.1 to -26.1 dBm for Pol-V. In contrast to wireless services, power reaches -24.7 to -22.4 dBm and -24.1 to -22.1 dBm. Therefore, the receiver sensitivity difference between these services lies between ~ 3 to ~ 4 dBm. In the insets, for the fixed received power, the eye diagrams (the case of ONU1) within the time window of one bit period also display the deterioration differences for successive wired

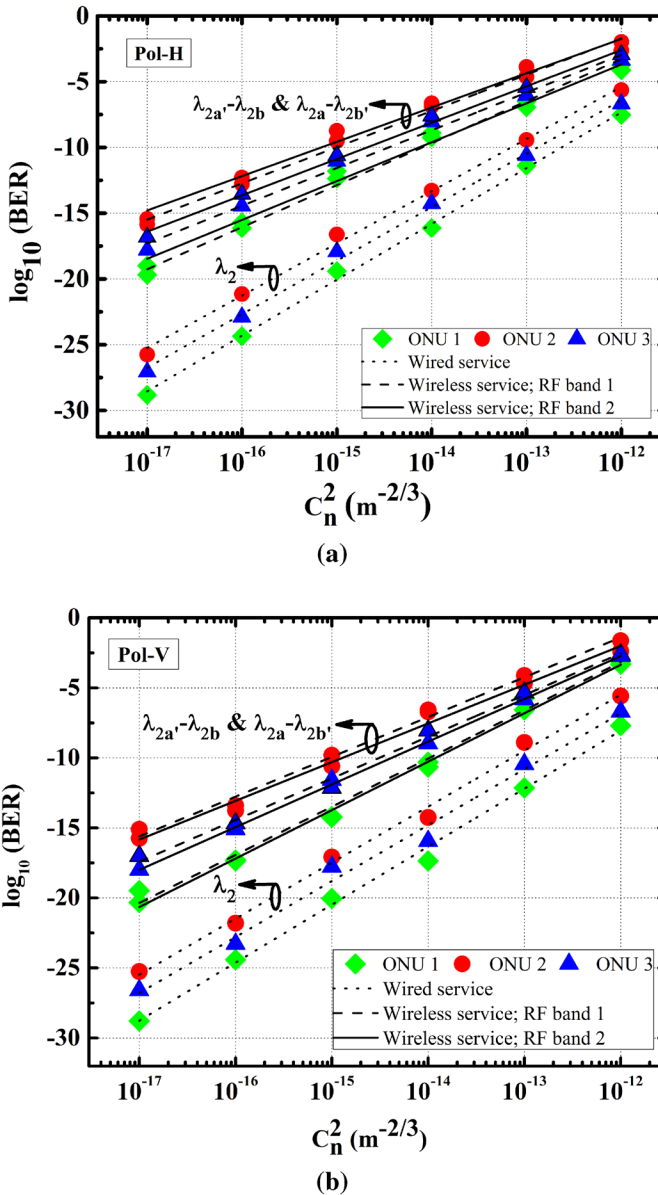


Fig. 7 BER of wired and wireless scenarios against C_n² for a Pol-H, b Pol-V

and wireless services. Although, it has been measured for the case of ONU1, same transition is likely to be observed for the rest of the cases.

Figure 7a, b show the effect of turbulence ($C_n^2 = 10^{-17}m^{-2/3}$ to $10^{-12}m^{-2/3}$) on 400 m FSO link. Though, both SOPs offer approximate similar performance, the significant impact of a crosstalk interference is observed on intermediate channel/bands ($\lambda_2/\lambda_{2a'} - \lambda_{2b}$, $\lambda_{2a} - \lambda_{2b'}$) compared to outer channels/bands.

5 Conclusion

By upgrading the conventional FSO link, deployment of simultaneous wired and wireless services is proposed to be spread over the existing PON network in urban or highly congested areas. In this approach, a 400 m/18 \times 2.5 Gb/s FSO system is designed by interleaving baseband and multiband RF signals in DWDM architecture. To double the spectral efficiency, two distinct orthogonal SOPs are used for transmitting independent data streams in a single channel. The BER performance with respect to received optical power and turbulence strength on FSO link is evaluated. Results attribute that, intermediate channels/bands require a bit more spectral spacing to prevent overlapping induced congestion compared to outside channels/bands. In addition, for BER of 10^{-9} , wireless services require notable power than wired services due to the additional loss in an RF signal coverage.

Acknowledgements This work was supported by R and D division of Sardar Vallabhbhai National Institute of Technology, Surat, India under ECED/Annual plan/1104/3624/2014-15 and 1673/2014-15.

References

- Aldouri, M.Y., Aljunid, S., Fadhil, H.A.: Study of the ocdma transmission characteristics in fso-ftth at various distances, outdoor. *J. Opt. Commun.* **34**(2), 127–133 (2013)
- Badar, N., Jha, R.K.: Performance comparison of various modulation schemes over free space optical (fso) link employing gamma-gamma fading model. *Opt. Quant. Electron.* **49**(5), 192 (2017)
- Badar, N., Jha, R.K., Towfeeq, I.: Performance analysis of an 80 (8 \times 10) gbps rz-dpsk based wdm-fso system under combined effects of various weather conditions and atmospheric turbulence induced fading employing gamma-gamma fading model. *Opt. Quant. Electron.* **50**(1), 44 (2018)
- Bakaul, M., Nirmalathas, A., Lim, C., Novak, D., Waterhouse, R.: Efficient multiplexing scheme for wavelength-interleaved DWDM millimeter-wave fiber-radio systems. *IEEE Photon. Technol. Lett.* **17**(12), 2718–2720 (2005)
- Chaudhary, S., Lin, B., Tang, X., Wei, X., Zhou, Z., Lin, C., Zhang, M., Zhang, H.: 40 gbps-80 ghz psk-mdm based ro-fso transmission system. *Opt. Quant. Electron.* **50**(8), 321 (2018)
- Ciaramella, E., Arimoto, Y., Contestabile, G., Presi, M., D'Errico, A., Guarino, V., Matsumoto, M.: 1.28 terabit/s (32 \times 40 gbit/s) wdm transmission system for free space optical communications. *IEEE J. Sel. Areas Commun.* **27**(9), 1639–1645 (2009)
- Dayal, N., Singh, P., Kaur, P.: Long range cost-effective wdm-fso system using hybrid optical amplifiers. *Wireless Pers. Commun.* **97**(4), 6055–6067 (2017)
- Devgan, P.S., Brown, D.P., Nelson, R.L.: Rf performance of single sideband modulation versus dual sideband modulation in a photonic link. *J. Lightw. Technol.* **33**(9), 1888–1895 (2015)
- Ghassemlooy, Z., Popoola, W., Rajbhandari, S.: *Optical Wireless Communications: System and Channel Modelling with Matlab®*. CRC Press, Boca Raton (2019)
- Ghosh, S., Basu, K., Das, S.K.: An architecture for next-generation radio access networks. *IEEE Network* **19**(5), 35–42 (2005)
- Giannetti, F., Luise, M., Reggiannini, R.: Mobile and personal communications in the 60 ghz band: A survey. *Wireless Pers. Commun.* **10**(2), 207–243 (1999)
- Hayee, M., Cardakli, M., Sahin, A., Willner, A.: Doubling of bandwidth utilization using two orthogonal polarizations and power unbalancing in a polarization-division-multiplexing scheme. *IEEE Photonics Technol. Lett.* **13**(8), 881–883 (2001)
- Hsueh, Y.T., Jia, Z., Chien, H.C., Yu, J., Chang, G.K.: A novel bidirectional 60-ghz radio-over-fiber scheme with multiband signal generation using a single intensity modulator. *IEEE Photonics Technol. Lett.* **21**(18), 1338–1340 (2009)
- Kaushal, H., Kumar, V., Dutta, A., Aennam, H., Jain, V., Kar, S., Joseph, J.: Experimental study on beam wander under varying atmospheric turbulence conditions. *IEEE Photon. Technol. Lett.* **23**(22), 1691–1693 (2011)

- Kim, I.I., Korevaar, E.J.: Availability of free-space optics (fso) and hybrid fso/rf systems. In: Optical Wireless Communications IV, International Society for Optics and Photonics **4530**, 84–96 (2001)
- Li, M., Chen, H., Yin, F., Chen, M., Xie, S.: Dwdm-based frequency-interleaved optical distributing system merging wired and wireless services. *IEEE Photon. Technol. Lett.* **21**(15), 1048–1050 (2009)
- Majumdar, A.K.: *Advanced Free Space Optics (FSO): A Systems Approach*, vol. 186. Springer, Berlin (2014)
- Majumdar, A.K., Ricklin, J.C.: *Free-Space Laser Communications: Principles and Advances*, vol. 2. Springer, Berlin (2010)
- Mallick, K., Mukherjee, R., Das, B., Mandal, G.C., Patra, A.S.: Bidirectional hybrid ofdm based wireless-over-fiber transport system using reflective semiconductor amplifier and polarization multiplexing technique. *AEU-Int. J. Electron. Commun.* **96**, 260–266 (2018)
- Mallick, K., Mandal, P., Mandal, G.C., Mukherjee, R., Das, B., Patra, A.S.: Hybrid MMW-over fiber/OFDm-fso transmission system based on doublet lens scheme and polmux technique. *Opt. Fiber Technol.* **52**, 101942 (2019)
- Mandal, G.C., Mukherjee, R., Das, B., Patra, A.S.: Bidirectional and simultaneous transmission of baseband and wireless signals over rsoa based wdm radio-over-fiber passive optical network using incoherent light injection technique. *AEU-Int. J. Electron. Commun.* **80**, 193–198 (2017)
- Mandal, G.C., Mukherjee, R., Das, B., Patra, A.S.: A full-duplex wdm hybrid fiber-wired/fiber-wireless/fiber-VLC/fiber-IVLC transmission system based on a self-injection locked quantum dash laser and a rsoa. *Opt. Commun.* **427**, 202–208 (2018)
- Ni, W., Miyamoto, Y., Wakamori, K., Kazaura, K., Matsumoto, M., Higashino, T., Tsukamoto, K., Komaki, S.: Experimental study of atmospheric turbulence effects on rfsso communication systems. *Piers Online* **5**(1), 65–70 (2009)
- Sharma, V., Kaur, G.: High speed, long reach ofdm-fso transmission link incorporating ossb and otsb schemes. *Optik* **124**(23), 6111–6114 (2013)
- Soni, G.G., Tripathi, A., Mandloi, A., Gupta, S.: Effect of wind pressure and modulation schemes on rain interrupted optical wireless links under tropical climates. *Opt. Quant. Electron.* **51**(6), 172 (2019)
- Tripathi, A., Soni, G.G., Gupta, S., Mandloi, A.S.: Experimental investigation of wind and temperature induced scintillation effect on optical wireless communication link. *Optik* **178**, 1248–1254 (2019)
- Tsai, W.S., Lu, H.H., Li, C.Y., Lu, T.C., Liao, C.H., Chu, C.A., Peng, P.C.: A 20-m/40-gb/s 1550-nm ddb id-based fso link. *IEEE Photon. J.* **7**(6), 1–7 (2015)
- Yeh, C.H., Gu, C.S., Guo, B.S., Chang, Y.J., Chow, C.W., Tseng, M.C., Chen, R.B.: Hybrid free space optical communication system and passive optical network with high splitting ratio for broadcasting data traffic. *J. Opt.* **20**(12), 125702 (2018)
- Yong, S.K., Xia, P., Valdes-Garcia, A.: *60GHz Technology for Gbps WLAN and WPAN: from Theory to Practice*. Wiley, New York (2011)
- Yu, J., Jia, Z., Yi, L., Su, Y., Chang, G.K., Wang, T.: Optical millimeter-wave generation or up-conversion using external modulators. *IEEE Photon. Technol. Lett.* **18**(1), 265–267 (2005)
- Zhang, R., Ma, J.: Full-duplex hybrid pon/rof link with 10-gbit/s 4-QAM signal for alternative wired and 40-GHz band wireless access based on optical frequency multiplication. *Optik* **138**, 55–63 (2017)

Publisher's Note Springer Nature remains neutral with regard to jurisdictional claims in published maps and institutional affiliations.